

Active vibration control of an inertial actuator subject to broadband excitation

S Camperi, M Ghanchi-Tehrani, M Zilletti and S J Elliott

Institute of Sound and Vibration Research, University of Southampton, Southampton SO17 1BJ, UK

E-mail: sc4r14@soton.ac.uk

Abstract. Active vibration control has been widely used in many engineering applications in order to minimise vibrations in structures, when subjected to broadband random disturbances. Feedback control in the form of velocity feedback is considered in this paper, which generates a damping force proportional to the velocity. The control gain is tuned in such a way to minimise the kinetic energy of the system. In this paper, an inertial actuator excited by a random voltage is considered and an active control is implemented. The dynamic equations of the system are derived and the response is obtained with and without control. The stability of the system is analysed using the Nyquist plot. The response of the actuator is obtained from time domain simulations using Matlab. The effect of the control gains are also investigated on the responses. Energy analysis shows how the energy in the system decreases by increasing the feedback gain up to a stability limit.

1. Introduction

Vibrations may occur in structural dynamic as undesired consequence of certain operative conditions and their effect can span from being a discomfort source up to damaging the whole structure. Electromagnetic actuators can be implemented in structural dynamic for vibration control purposes and enhancing system stability [1]. The objective of noise reduction through electromagnetic transducers is to limit undesired vibrations applying an external force obtained, in a straightforward solution, as a feedback control [2, 3]. Kinetic energy of the structure is analysed as noise level index and its minimisation is pursued by means of an active damping feedback control proportional to the plant local velocity [4, 5].

The amount of force available makes these devices act locally which suggests the use of multiple actuators in centralised [3] and decentralised [6] configurations. Centralised control allows selective mode control of the structure but it requires an accurate modelling of the response, making the implementation complex and the design specifically customised for the system analysed. Moreover, the control forces depend on the feedback of every signal from each unit, therefore the disruption of even just a channel can lead to the instability of the whole system. On the other hand, decentralised control is based on the independence of each unit and failure of one of one unit does not affect the others. However, this approach is less selective and its tuning is more complex.

Electromagnetic actuators can be implemented on a structure as devices reacting between the plant and an external support [7] or as inertial actuators [8] self-supported by the structure. The former ones need an external support to react off, thus they introduce less modifications in



the plant dynamic allowing a robust and more straightforward control. The latter ones, instead, introduce a more complex dynamic interaction given by the moving mass of the inertial actuator with risk of instability, nevertheless they represent a more flexible solution.

Minimisation of the global plant kinetic energy provides valuable performance in terms of vibration reduction [5], but it cannot be adopted when the information about the global structure is not available such as in decentralised control. For this reason, alternative solutions have been analysed to tune the feedback gain in such a way to obtain valuable results in decentralised architectures. One possible solution when only local information are available is the maximisation of energy absorbed by the transducers from the structure [9] and, as it has been shown [4], for a single degree of freedom system with ideal constant velocity feedback gain, it corresponds analytically to the minimisation of the kinetic energy.

This paper is structured in six main sections. Section 2 describes the mathematical model of a general electromechanical inertial actuator, a velocity feedback control loop is then introduced and kinetic energy is analysed. Section 3 presents the set-up adopted in the experiment which has been used for the model identification discussed in Section 4. Finally, active control and stability issue are analysed in Section 5.

2. Mathematical model

The electromagnetic inertial actuator can be described as a voice coil transducer [1], which allows the transformation of energy between a mechanical and an electrical system. The device consists of a permanent magnet with magnetic flux density B , and a coil of length l , free to move axially within the gap.

Assuming B to be constant with respect to the axial coordinate, based on Faraday's law, a voltage e is generated into the coil proportional to the velocity v of coil with respect to the magnet,

$$e = -Blv. \quad (1)$$

Secondly, according to the Lorentz force law, a force f_e is generated between the coil and the magnet as a current i flows through the coil.

$$f_e = Bli. \quad (2)$$

Notice that, from Equations (1), (2) the first law of thermodynamic holds, i.e. there is equilibrium between the mechanical power absorbed and the electrical power delivered and vice versa.

$$f_e v + ei = 0. \quad (3)$$

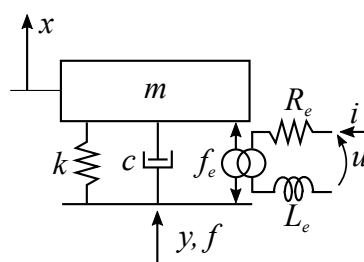


Figure 1: Scheme of the SDOF inertial actuator.

From the mechanical point of view, the transducer can be described as single degree of freedom system with a moving mass m , a stiffness k and a damping c , excited by a force from the electrical system f_e generated by the electromagnetic interaction as expressed in Equation (2). Considering x and y as absolute displacements of the moving mass and of the base, the dynamic equation of the system can be written as,

$$m\ddot{x} + c(\dot{x} - \dot{y}) + k(x - y) = Bli. \quad (4)$$

On the other hand, in the electrical system, taking into account the inducted voltage from Equation (1), a voltage u can be measured at the ends of the coil which is equal to

$$u = Bl(\dot{x} - \dot{y}) + R_e i + L_e \frac{di}{dt}, \quad (5)$$

where R_e and L_e are the internal resistance and inductance of the loop. The force transmitted to the ground f by the inertial actuator is proportional to the acceleration of the moving mass.

$$f = -m\ddot{x}. \quad (6)$$

A two-port network analysis of the system can be performed [10], in which the force transmitted to the ground f and the voltage applied u are evaluated with respect to the current flowing through the coil and the velocity of the base \dot{y}

$$f = Ti - Z_m \dot{y}, \quad (7)$$

$$u = Z_e i + T \dot{y}. \quad (8)$$

where T , Z_m and Z_e are the transduction coefficient between the mechanical and the electrical system, the mechanical impedance and the electrical base impedance respectively.



Figure 2: Experimental set-up of the inertial actuator “Data Physics IV40” fixed on the test-rig through a force cell with an accelerometer mounted on the moving part.

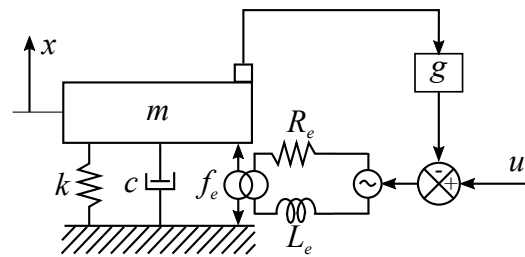


Figure 3: Scheme of the inertial actuator with velocity feedback control.

Assuming the system is linear, the Laplace Transform can be applied to Equations (4) and (5) leading to the following set of equations for T , Z_m and Z_e .

$$T = \frac{-mBls^2}{ms^2 + cs + k}, \quad (9)$$

$$Z_m = \frac{ms(cs + k)}{ms^2 + cs + k}, \quad (10)$$

$$Z_e = R_e + sL_e + \frac{s(Bl)^2}{ms^2 + cs + k}. \quad (11)$$

From the Equations (7) and (8), the particular case in which the inertial actuator is grounded can be derived. The forward transfer function M between the input voltage u and the moving mass velocity \dot{x} can be written, according to Equations (6), (7) and (8), as

$$M(s) = \frac{\dot{X}(s)}{U(s)} = \frac{Bl s}{(ms^2 + cs + k)(L_e s + R_e) + (Bl)^2 s}. \quad (12)$$

From Figure (3), a feedback control is added to the system with feedback transfer function H which is constant and equal to a gain g . According to Figure (4), the closed-loop transfer function Y in the Laplace domain is then

$$Y(s) = \frac{M(s)}{1 + M(s)H}. \quad (13)$$

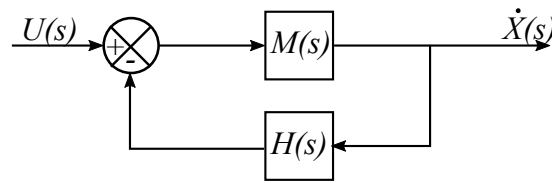


Figure 4: Scheme of the feedback control system.

Broadband excitation is considered as a general form of excitation for many practical applications. Once the input is assumed to be stationary, the output will be in the same form. Global kinetic energy \bar{E}_k can be analysed as an index of the dynamic behaviour of the system. As the energy tends to infinity, the time window considered of length T increases and the average value is analysed

$$\bar{E}_k = \frac{1}{T} \int_{-1/T}^{1/T} \frac{1}{2} m \dot{x}^2(t) dt. \quad (14)$$

According to Parseval's theorem, Equation (14) can be written in the frequency domain as

$$\bar{E}_k = \frac{1}{2} m \lim_{T \rightarrow \infty} \frac{1}{T} \int_{-\infty}^{\infty} |\dot{X}(f)|^2 df, \quad (15)$$

where $\dot{X}(f)$ is the Fourier Transform of the velocity signal $\dot{x}(t)$. Finally, if ergodicity of the input signal is assumed, the Expected value of the signals can be analysed leading to

$$\bar{E}_k = \frac{1}{2} m \int_{-\infty}^{\infty} S_{\dot{x}\dot{x}}(f) df = \frac{1}{2} m \int_{-\infty}^{\infty} |M(f)|^2 S_{uu}(f) df, \quad (16)$$

where $S_{\dot{x}\dot{x}}$ and S_{uu} are the Power Spectral Density of the velocity \dot{x} and input voltage u . Considering a white noise as input, S_{uu} is constant and can be brought out from the integral so that Equation (16) can be rewritten as

$$\bar{E}_k = \frac{1}{2}mS_{uu} \int_{-\infty}^{\infty} |M(f)|^2 df, \quad (17)$$

According to Newland [11], the integral of Equation (17) can be solved with respect to g as,

$$I = \int_{-\infty}^{\infty} |M(f)|^2 df = \frac{A_0}{B_1g + B_0}, \quad (18)$$

where A_0 , B_0 and B_1 are given in Table (1). As can be seen from the Equation (18), global kinetic energy decreases as the control gain g becomes larger, proving the unconditional stability of the system.

Table 1: Parameters of I in Equation (18)

Parameter	Espression
A_0	$kR_e(Bl)^2$
B_0	$kR_e \left\{ [(Bl)^2 + cR_e + kL_e](mR_e + cL_e) - kR_emL_e \right\}$
B_1	$kR_e(mR_e + cL_e)Bl$

3. Experimental set-up

The experimental set-up is shown in Figure (2). An inertial actuator “Data Physics IV40” is attached perpendicularly to the test-rig via a thin layer of adhesive wax. Consistently with what has been presented in the mathematical model, the transducer is driven by a voltage and moving mass dynamic and the force transmitted to the ground are analysed. Secondly, a velocity feedback control is implemented which performance and stability are evaluated. Open-loop transfer function analysis allows the parameters identification, then a comparison between experimental and mathematical model of the closed-loop transfer function is presented.

Input signal u is provided from a Simulink[®] model through dSPACE[®] platform. Low-pass filter is included after the digital to analogical (DA) conversion of the signal in order to avoid aliasing. Finally, a power amplifier (Data Physics PA30E) magnifies the signal from the filter providing energy to the inertial actuator.

An accelerometer, mounted on the moving part of the transducers, feeds-back the velocity of the moving mass into the Simulink[®] model through a B&K type 2635 charge amplifier. Similarly, the transmitted force signal from the load cell mounted in between the inertial actuator and the test-rig is fed-back into the Simulink[®] by means of another charge amplifier.

The global transfer function G between the input voltage and the moving mass velocity is considered in Equation (13) rather than M . Since G includes a DA conversion and a filter, delay is introduced into the system [12], and the unconditional stability is no longer guaranteed.

4. Identification

Model parameters identification is performed driving the inertial actuator fixed to the ground with an input voltage u and measuring the current i and the force transmitted f .

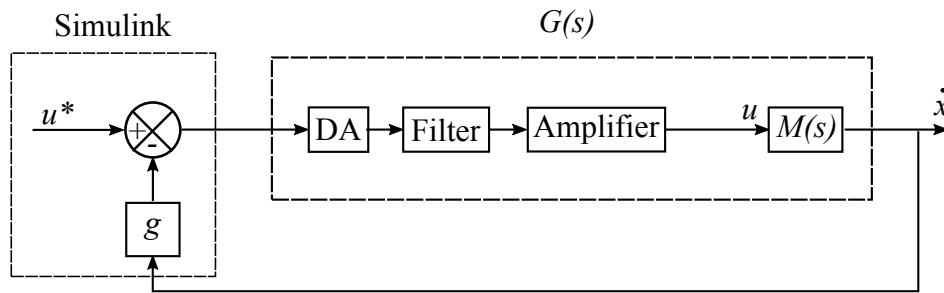


Figure 5: Scheme of the feedback control digital system.

From Equation (7), electrical base impedance Z_e and transduction coefficient T can be obtained as

$$T = \frac{F(s)}{I(s)}, \quad (19)$$

$$Z_e = \frac{U(s)}{I(s)}. \quad (20)$$

From Equation (9), model identification is performed and a comparison with the mathematical model is presented in Figures (7), (6). Table (2) shows the parameters used, where the values in bold have been directly measured, while the values in italic come from the identification.

From the analysis of T , if the system is not highly damped, natural frequency f_n and damping ratio ξ of the mechanical system are known from the resonance peak, instead the voice coil coefficient Bl is the horizontal asymptote. According to Figure (7), natural frequency f_n occurs around 40 Hz, where the force transmitted to the ground per unit of current has a maximum. For exciting frequencies below the resonance, low-magnitude and in-phase force is generated, while above the resonance a constant force is provided in phase opposition, thus the inertial actuator can be seen as an high-pass filter which, at high frequencies, behaves as an ideal force generator.

On the other hand, the electrical parameters can be obtained from the electrical base impedance Z_e . Below the resonance, the frequency response can be considered equal to the internal resistance R_e that can be also directly measured. The oblique asymptote at high frequency, instead, is equal to the internal inductance of the coil L_e . According to Figure (6), it can be noticed that a peak is present around the natural frequency due to the coupling of the electrical system with the mechanical part.

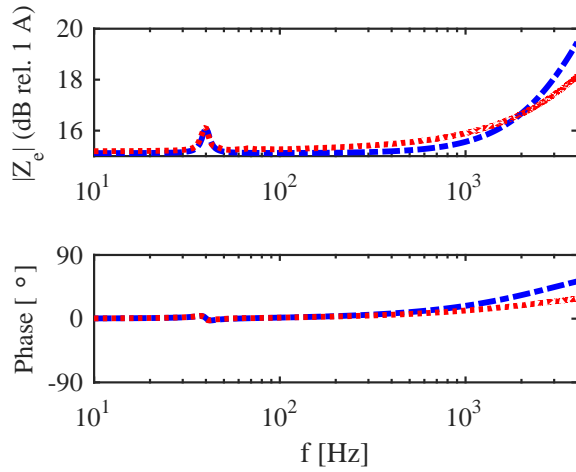


Figure 6: Comparison between analytical (*dash-dotted blue*) and experimental (*dotted red*) bode diagram of the electrical base impedance Z_e .

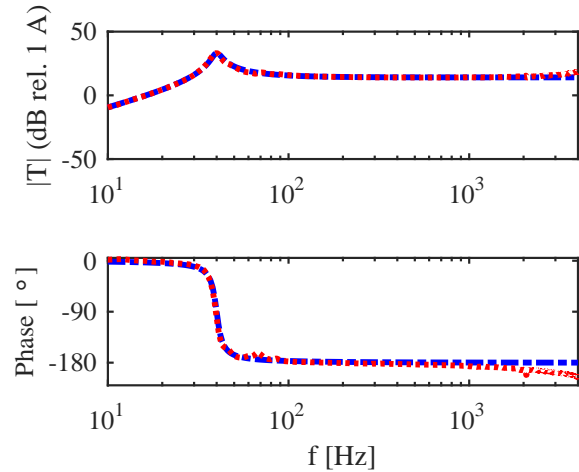


Figure 7: Comparison between analytical (*dash-dotted blue*) and experimental (*dotted red*) bode diagram of the transduction coefficient T .

Table 2: Parameters of the electromagnetic inertial actuator DataPhysics IV40

Parameter	Value	Unit
Moving mass (m)	1.35	kg
Natural frequency (f_n)	40	Hz
Damping ratio (ξ)	0.05	-
Voice coil coefficient (Bl)	5.6	NA ⁻¹
Electrical resistance (R_e)	1.7	Ω
Electrical inductance (L_e)	0.298	mH

5. Active control experiments

The moving mass velocity of the inertial actuator is analysed with respect to a voltage input as forward transfer function M of the mathematical model introduced. According to Equation (12), a comparison between experimental results and analytical model is presented in Figures (8a) and (8b).

Closed-loop stability of the system presented in (13) can be evaluated through the Nyquist plot in Figure (8b). Instability occurs when the open-loop transfer function MH cross the point $(-1,0)$ on the Nyquist plot. As can be seen, considering a constant feed-back transfer function $H = g$, the system is unconditionally stable for any positive value of the feedback gain. However, if the control is performed through the Simulink[®] model as presented above, global transfer function G has to be considered rather than M , which allows describing the digital system generated. As shown in Figure (5), according to Franklin [12], a sampled and quantized voltage u^* is converted by the dSPACE[®] in an analogical signal with a phase delay proportional to the sampling frequency which, in this work, has been set at 10 kHz. Analogical low-pass filter has been then implemented to avoid aliasing for frequencies above the Nyquist frequency, i.e. half the sampling frequency. In order to minimise the delay introduced by the filter, the pass-band frequency has been set at 4 kHz. Finally a power amplifier has been introduced, with a linear response in the frequency range considered which allows describing it as a simple gain being the phase delay negligible.

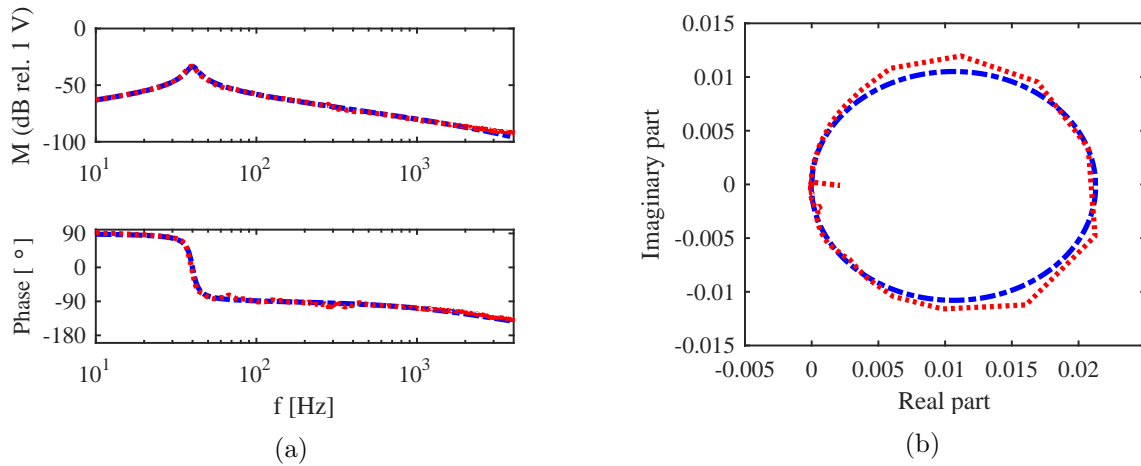


Figure 8: Bode diagram (a) and Nyquist plot (b) comparison between analytical (*dash-dotted blue*) and experimental (*dotted red*) results of the forward transfer function M .

As shown in Figure (9a), a larger delay at high frequencies with respect to M is present mostly

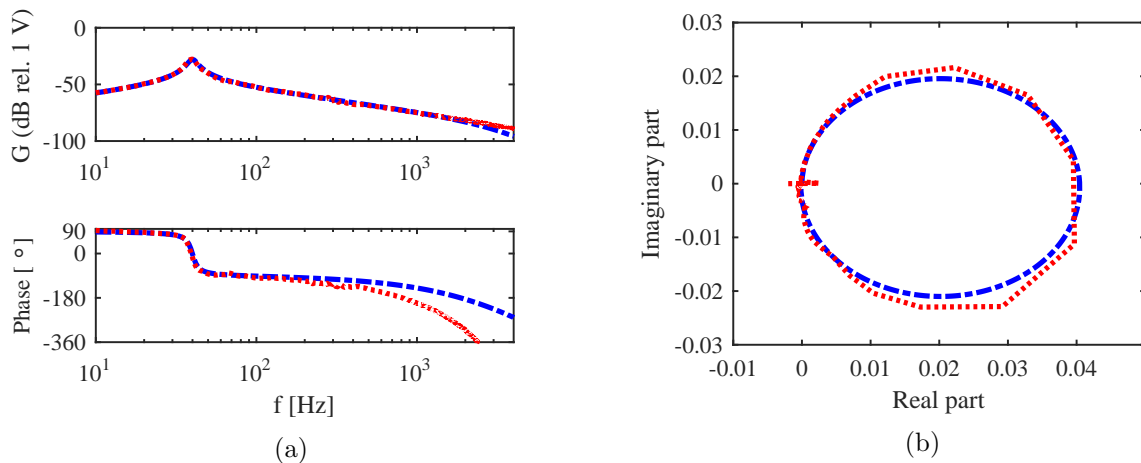


Figure 9: Bode diagram (a) and Nyquist plot (b) comparison between analytical (*dash-dotted blue*) and experimental (*dotted red*) results of the global forward transfer function G .

due to the presence of the filter and the DA converter. Differences between mathematical and experimental results are due to the filter idealisation.

As clarified in Figure (9b), high frequency delay causes the system to be not unconditionally stable, thus a maximum gain can be defined. Figure (10) shows a comparison between mathematical model and experimental results of the closed-loop transfer function Y . A decrement of moving mass velocity can be noticed as the control gain g increases, while instability at higher frequencies rises.

Global kinetic energy can be evaluated both numerically and experimentally from Figure (10) as integral of the area underneath the closed-loop transfer function Y . As shown in Figure (11), the moving mass global kinetic energy decreases as the control gain g is increased. Furthermore, a comparison is proposed with the analytical results presented in Equation (18). The difference between results is due to the fact that mathematical model is unconditionally stable and it takes into account all the frequency domain whereas in the experimental and numerical model just a finite frequency range can be considered.

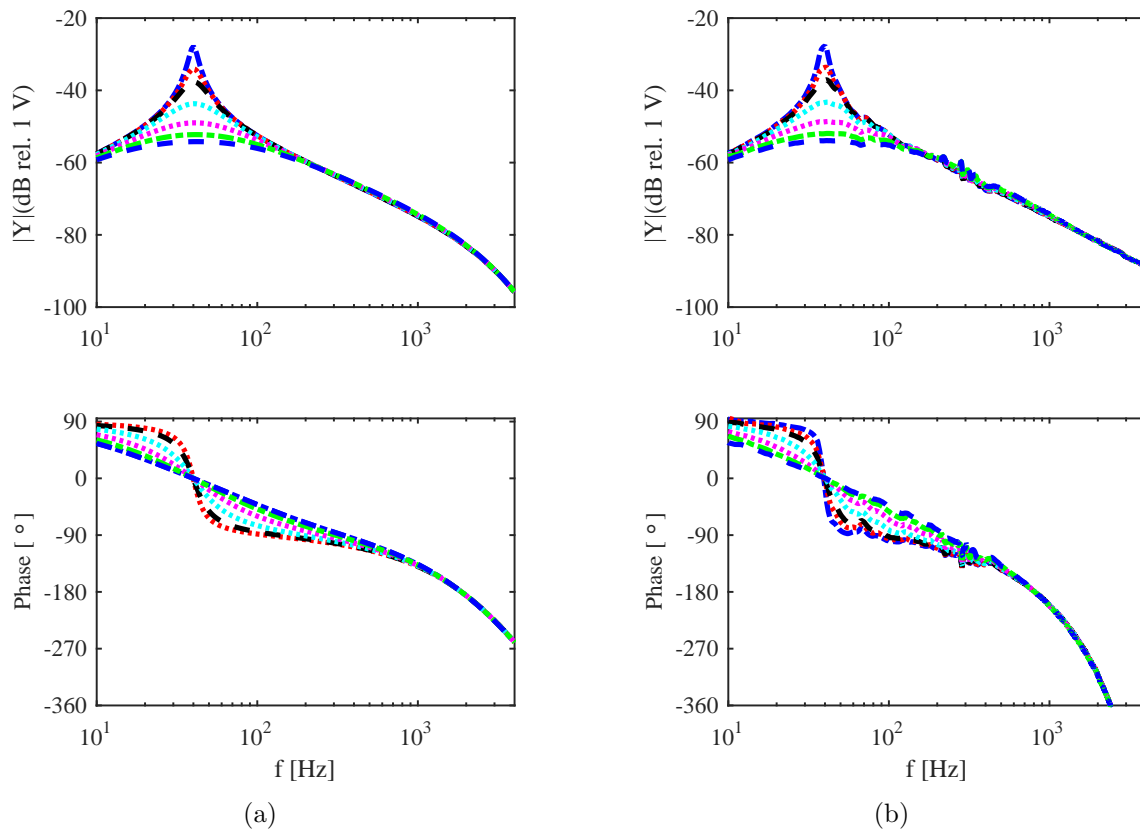


Figure 10: Analytical (a) and experimental (b) bode diagram of the closed-loop transfer function Y for different values of g : 0% (*dash-dotted blue*), 5% (*dotted red*), 10% (*dashed black*), 25% (*dotted cyan*), 50% (*dotted magenta*), 75% (*dash-dotted green*), 90% (*dashed blue*).

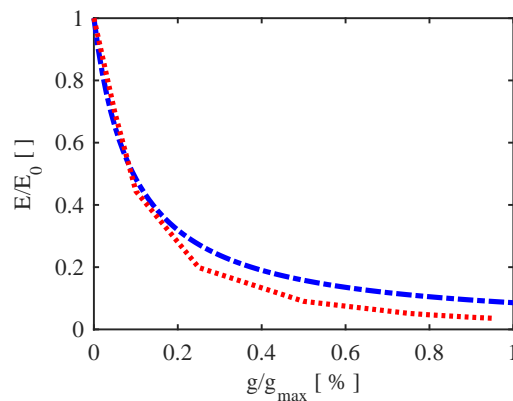


Figure 11: Comparison between analytical (*dash-dotted blue*) and experimental (*dotted red*) global kinetic energy of the controlled SDOF with respect to the feedback control gain.

6. Conclusions and future work

This paper presents experimental and analytical results of a velocity feedback control loop of an inertial actuator driven by an input voltage source. Unconditional stability of the mathematical model is proved and conditional stability of the digital system is analysed pointing out the

maximum gain value.

The formulation presented in this paper can be exploited to investigate structural dynamic problems such as control of structures where inertial actuators can be introduced to minimise global kinetic energy of the plant. Active control can be obtained tuning the feedback gain in such a way to maximise energy absorption but instability issues need to be taken into account. For future work, active control of a thin plate will be considered with decentralised control strategies in which multiple inertial actuators will be considered and the system stability will be investigated.

Acknowledgments

This research work was supported by the European Commission as “Marie Skłodowska-Curie Fellowship for Early Stage Research” program through the “Initial Training Network” (ITN) within the seventh framework “Advanced Training and Research in Energy Efficient Smart Structures” (ANTARES) project (Grant Agreement 606817).

- [1] Preumont A 2012 *Vibration control of active structures: an introduction* vol 50 (Springer Science & Business Media)
- [2] Meirovitch L 1990 *Dynamics and control of structures* (John Wiley & Sons)
- [3] Elliott S 2000 *Signal processing for active control* (Academic press)
- [4] Zilletti M, Gardonio P and Elliott S J 2014 *Journal of Sound and Vibration* **333** 4405–4414
- [5] Gardonio P, Miani S, Blanchini F, Casagrande D and Elliott S 2012 *Journal of sound and vibration* **331** 1722–1741
- [6] Baumann O N and Elliott S J 2006 *Proceedings of the Sixth International Symposium on Active Noise and Vibration Control, ACTIVE 2006* cD-ROM
- [7] Zilletti M, Elliott S J and Gardonio P 2010 *Journal of Sound and Vibration* **329** 2738–2750
- [8] Rohlfing J, Gardonio P and Elliott S 2011 *Journal of Sound and Vibration* **330** 4661–4675
- [9] Elliott S, Zilletti M and Gardonio P 2010 *Recent Advances Structural Dynamics: Proceedings of the X International Conference* (University of Southampton)
- [10] Elliott S J and Zilletti M 2014 *Journal of Sound and Vibration* **333** 2185–2195
- [11] Newland D E 2012 *An introduction to random vibrations, spectral & wavelet analysis* (Courier Corporation)
- [12] Franklin G F, Powell J D and Workman M L 1998 *Digital control of dynamic systems* vol 3 (Addison-wesley Menlo Park)